Biomass burning and volcanic ash characterization at Centro de Investigaciones en Láseres y Aplicaciones, Buenos Aires, Argentina

Pablo Roberto Ristori, Lidia Ana Otero,
CEILAP (CITEDEF-CONICET), UMI-IFAECI-CNRS 3351
Juan B. de La Salle 4397 - B1603ALO - Villa Martelli, Buenos Aires, Argentina
Tel: +54 11 47098100 ext 1410, Fax: +54 11 47098122, E-mail: pablo.ristori@gmail.com
and **Juan Vicente Pallotta, Ezequiel Eduardo Pawelko, Eduardo Jaime Quel**
CEILAP (CITEDEF-CONICET), UMI-IFAECI-CNRS 3351
Juan B. de La Salle 4397 - B1603ALO - Villa Martelli, Buenos Aires, Argentina
Tel: +54 11 47098100 ext 1410, Fax: +54 11 47098122, E-mail: pablo.ristori@gmail.com

SUMMARY

Biomass burning events and volcanic ash transport measurements from a multi-wavelength backscatter LIDAR at Centro de Investigaciones en Láseres y Aplicaciones, CEILAP (CITEDEF-CONICET), (34.5° S, 58.5° W), Buenos Aires, Argentina are studied to characterize their optical properties. The lidar system operating at this place has the first three harmonics of a Nd:YAG laser and collects Raman returns from nitrogen and water vapor. Different aerosol layers were separated from the total acquisition and studied alone to characterize their optical properties at different wavelengths. Intended products are the backscatter coefficient and the color ratio. In addition a comparison between layers is performed, trying to determine their similarity. This method has the final goal of parameterizing the basic parameters of biomass burning originated aerosols and volcanic ashes transported over important distances.

Key words: Biomass burning, volcanic ash, Lidar, Color Ratio

INTRODUCTION

Lidar is a valuable tool to determine the presence of atmospheric aerosols and their telemetry. In some cases it can also retrieve extensive properties like the aerosol optical depth of these layers at the lidar measuring wavelength. However, even if important efforts have been done to determine aerosol microphysics [Muller et al, 1999], up to date aerosol type still remains a difficult to determine using this instrument.

This paper studies the lidar signals to retrieve the corrected aerosol attenuated backscatter and the attenuated aerosol color ratio for different aerosol intrusion events. The first one is the recent volcanic ash intrusion event at Buenos Aires due to the eruption of Puyehue Cordon del Caulle Volcano and the second is a late winter – early spring biomass burning transport at Buenos Aires. While the first parameter indicates the aerosol extensive properties, the second one is more related to their intensive properties and it is important to characterize the aerosol type.

SYSTEM DESCRIPTION

The Coaxial Multiwavelength Raman Lidar System (MWRLS) [Otero et al., 2011a] was conceived to monitor range-resolved aerosol optical properties from the IR to the near UV spectral region in the whole troposphere. Its emission system is a solid state Nd:YAG laser emitting its fundamental, doubled and tripled emission lines. An *f/2*, 1 m focal length Newtonian telescope, focus the backscattered signal into 1 mm diameter optical fiber that transmits the light to a dichroic/interference filter-based polychromator unit. In this way, three elastic wavelengths (1064 nm, 532 nm and 355 nm) and three Raman wavelengths (Nitrogen Raman backscattered signal from 532

nm and 355 nm, and Water Vapor Raman backscattered signal from and 355 nm) are measured at 7.5 m and 10 s bin intervals.

METHODS

The aerosol study presented in this paper uses 355 nm and 532 nm backscattered profiles as their aerosol signature can be easily compared to the molecular profile. Infrared (1064 nm) backscatter is mostly used to indicate the aerosol presence in a specific region especially when aerosol loads are difficult to detect on the other channels. The attenuated scattering ratio at wavelength λ (Vaughan et al., 2005) is calculated from the elastic lidar signals to the attenuated molecular backscatter β'^{λ}_{m} ratio; this last obtained from the radiosonde – derived molecular backscatter $\beta^{\lambda}_{m}(z)$ and extinction $\alpha^{\lambda}_{m}(z)$. Constant k is assumed to set this ratio to unity where the signal matches pure molecular backscatter at a given height.

$$R' = \frac{\beta'^{\lambda}_{Total}(z)}{\beta'^{\lambda}_{m}(z)} = k \frac{signal(z).z^2}{\beta^{\lambda}_{m}(z)\exp\left(-2\int_0^z \alpha^{\lambda}_{m}(\zeta)d\zeta\right)} \quad (1)$$

We use this calculation to approximate the corrected aerosol attenuated backscatter as:

$$\beta'^{\lambda}_{aer} = (R-1)\beta^{\lambda}_{mol} \quad (2)$$

From this value it is possible to calculate the attenuated aerosol color ratio here defined as:

$$\chi'^{\lambda_1}_{\lambda_2}(z) = \frac{\beta'^{\lambda_1}_{aer}(z)}{\beta'^{\lambda_2}_{aer}(z)}$$ (3)

RESULTS

The days studied are the 7 – 8 June 2011 in which a volcanic ashes intrusion event was detected and a biomass burning event the 9 September 2010.

Figure 1 shows the attenuated total backscatter in arbitrary units and logarithmic scale. A reference to this period can be found at [Otero et al, 2011b]. Cloud coverage was important and made difficult the analysis using other instrumentation than the lidar.
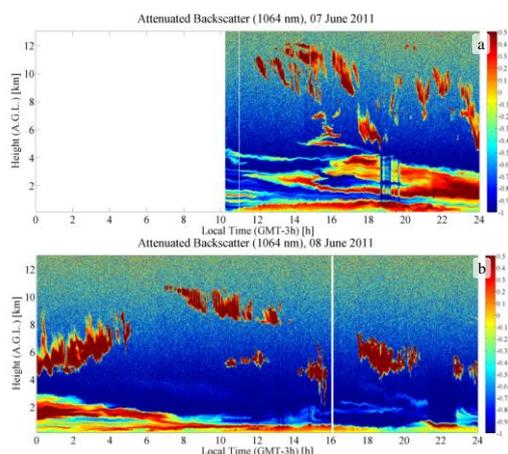
Figure 1. Aerosol Attenuated Total Backscatter Profile measured at 1064 nm for the (a) 07 June 2011 and (b) 08 June 2011. Boundary layer aerosols, volcanic aerosols mid-level and high level clouds can be observed.

Tree periods were studied for the first day averaging during 1 hour. For them the attenuated backscatter and attenuated scattering ratio was plotted versus height. The first (figure 2) was at noon, the second (figure 3) in the early afternoon, and the third (figure 4) during the night.

As it can be seen on those figures, the attenuated aerosol color ratio χ' reaches values from 0.75 to 1 for volcanic ashes and 0.5 for local aerosols inside the boundary layer. These values are independent of the aerosol load which confirms that the assumption of χ' as an intensive aerosol property was valid even knowing that aerosol extinction parameters at both wavelengths were not eliminated from the equation. This effect can be seen at the positive slope of χ' on figure 4 consequence of the two way 532 nm to 355 nm transmission ratio.

During nighttime, 10 minute average signals were taken to perform an extensive study of these two parameters in a period of time between 0 h and 7 h.

Figures 5 show the aerosol attenuated backscatter at 532 nm at which local aerosols are found along the first kilometer, a strong backscatter volcanic plume is above this layer and, from midnight to 4 am, a cloud layer is clearly distinguishable above 4.5 km.

Figure 6 shows the attenuated aerosol scattering ratio displaying the difference between the low altitude city aerosols (0.2 to 0.6) and the high altitude volcanic ashes (0.7 to 1) and clouds (1 – 1.2)
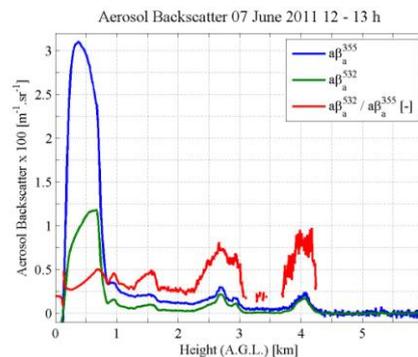
Figure 2. Aerosol attenuated backscatter (aβ$_a$) and aerosol color ratio (χ'). Below 2 km χ is below 0.5 while for the layers above 2 km χ' reaches values of 0.75 to 1.
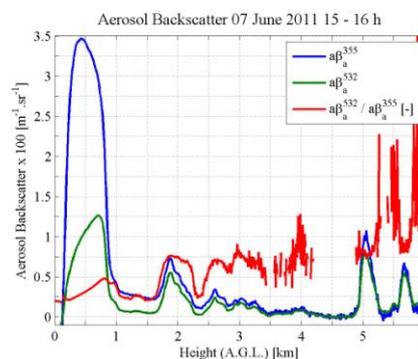
Figure 3. Aerosol attenuated backscatter (aβ$_a$) and color ratio (χ'). In presence of aerosol layers above 1.5 km, χ' reaches 0.75. Some spikes above these values are due to low aerosol values making undetermined the value of χ'.
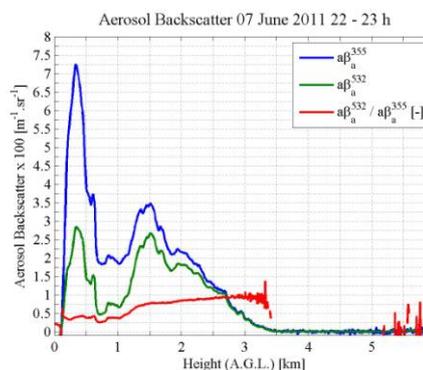
Figure 4. Aerosol attenuated backscatter (aβ$_a$) and scattering ratio (χ'). High aerosol loads do not affect the value of χ' which is almost the same as previous figures above 1 km.

The final part of this study analyzes the biomass burning event measured at Buenos Aires the 09 September 2010. The record of more than 7 hours is presented on figure 7.

As seen on figure 8 the aerosol attenuated backscatter values are much lower than in the previous case. The lower aerosol layer remains quite stable during the day and the convective activity is only evidenced in the first two hundred meters.

Figure 9 shows values of about 0.5 – 0.6 in the presence of biomass burning event. For lower altitudes these values are close to 0.2 to 0.4. The increasing values close to 1 km can be due to water vapor condensation that could be seen at the top of the first aerosol layer in the 1064 nm attenuated backscatter profile.
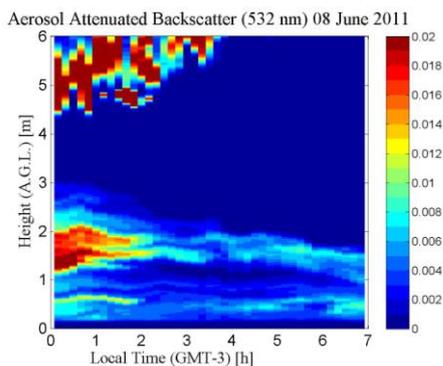
Figure 5. Ten minutes averaged aerosol attenuated backscatter. Stratified aerosol layers and clouds are present over the whole period.
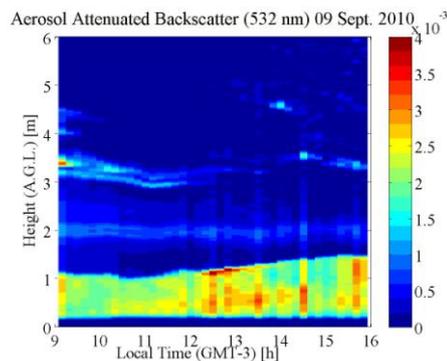

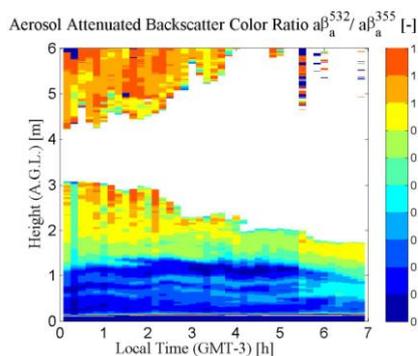**Figure 8. Ten minutes averaged aerosol attenuated backscatter. The aerosol loads are much lower than in figure 5**

Figure 6. Ten minute averaged aerosol attenuated color ratio. The color code can be used to identify the concentration-independent aerosol type.
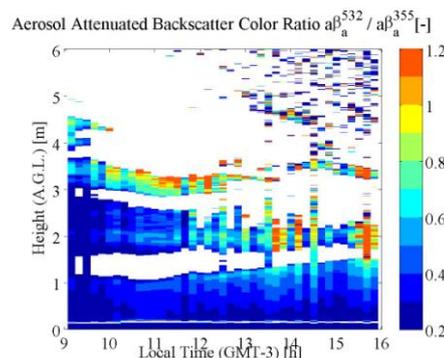

Figure 9. Ten minute averaged aerosol attenuated color ratio. Compared to figure 6 these calculated values for biomass burning are much lower than for volcanic ashes.
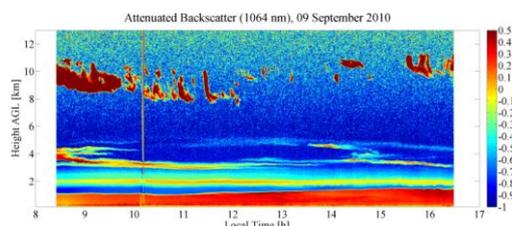
Figure 7. Aerosol Attenuated Total Backscatter Profile measured at 1064 nm for the 09 September, 2010.

CONCLUSIONS

Two different types of aerosols were studied using only the elastic wavelength capabilities of the Multiwavelength Raman Lidar System at the Lidar Division. The coaxial upgrade permitted to observe aerosol layers at heights as low as 200 meters. The rich information of the ultraviolet and visible channels permitted to see an almost constant color ratio behavior between aerosols of the same type independently of the time of the day or the aerosol concentration. I was also noticed that for different aerosol types the color ratio was significantly different making possible to separate aerosol type in the same event and at different events.

REFERENCES

Müller D., U. Wandinger, A. Ansmann, (1999) Microphysical Particle Parameters from Extinction and Backscatter Lidar Data by Inversion with Regularization: Theory, *Appl. Opt.* 38, 2346-2357.

Otero, L., P. Ristori, E. Pawelko, J. Pallotta, E. Quel (2011a), Six-Year Evolution of Multiwavelength Lidar System at CEILAP. V Workshop on Lidar Measurements in Latin America, *Opt. Pura Apl.,* 44, 13-18.

Otero, L., P. Ristori, E. Pawelko, J. Pallotta, E. Quel (2011b) The Puyehue-Cordón Caulle Volcanic Eruption, June 2011: Water Vapor, Atmospheric Boundary Layer and Aerosol Temporal Evolution in Buenos Aires, Argentina, *VI WLMA*, *Extended Abstract.*

Vaughan, M. A., D. M. Winker, K. A. Powell, (2005), CALIOP Algorithm Theoretical Basis Document, Part 2: Feature Detection and Layer Properties Algorithms, PC-SCI-202 Part 2